Physics Letters B 307 (1993) 237–246
North-Holland

PHYSICS LETTERS B

Measurement of $\Gamma_{b\bar{b}}/\Gamma_{had}$ from hadronic decays of the Z

L3 Collaboration

O. Adriani [n], M. Aguilar-Benitez [w], S. Ahlen [i], J. Alcaraz [o], A. Aloisio [z], G. Alverson [j], M.G. Alviggi [z], G. Ambrosi [ae], Q. An [p], H. Anderhub [as], A.L. Anderson [m], V.P. Andreev [ai], L. Antonov [am], D. Antreasyan [g], P. Arce [w], A. Arefiev [y], A. Atamanchuk [ai], T. Azemoon [c], T. Aziz [a,h], P.V.K.S. Baba [p], S. Bachmann [a], P. Bagnaia [ah], J.A. Bakken [ag], L. Baksay [ao], R.C. Ball [c], S. Banerjee [h], J. Bao [e], R. Barillère [o], L. Barone [ah], A. Baschirotto [x], R. Battiston [ae], A. Bay [q], F. Becattini [n], U. Becker [m,as], F. Behner [as], J. Behrens [as], Gy.L. Bencze [k], J. Berdugo [w], P. Berges [m], B. Bertucci [ae], B.L. Betev [am,as], M. Biasini [ae], A. Biland [as], G.M. Bilei [ae], R. Bizzarri [ah], J.J. Blaising [d], G.J. Bobbink [o,b], R. Bock [a], A. Böhm [a], B. Borgia [ah], M. Bosetti [x], D. Bourilkov [ab], M. Bourquin [q], D. Boutigny [d], B. Bouwens [b], E. Brambilla [z], J.G. Branson [aj], I.C. Brock [af], M. Brooks [u], A. Bujak [ap], J.D. Burger [m], W.J. Burger [q], J. Busenitz [ao], A. Buytenhuijs [ab], X.D. Cai [p], M. Capell [m], M. Caria [ae], G. Carlino [z], A.M. Cartacci [n], R. Castello [x], M. Cerrada [w], F. Cesaroni [ah], Y.H. Chang [m], U.K. Chaturvedi [p], M. Chemarin [v], A. Chen [au], C. Chen [f], G.M. Chen [f], H.F. Chen [r], H.S. Chen [f], M. Chen [m], W.Y. Chen [au], G. Chiefari [z], C.Y. Chien [e], M.T. Choi [an], S. Chung [m], C. Civinini [n], I. Clare [m], R. Clare [m], T.E. Coan [u], H.O. Cohn [ac], G. Coignet [d], N. Colino [o], A. Contin [g], X.T. Cui [p], X.Y. Cui [p], T.S. Dai [m], R. D'Alessandro [n], R. de Asmundis [z], A. Degré [d], K. Deiters [aq], E. Dénes [k], P. Denes [ag], F. DeNotaristefani [ah], M. Dhina [as], D. DiBitonto [ao], M. Diemoz [ah], H.R. Dimitrov [am], C. Dionisi [ah,o], L. Djambazov [as], M.T. Dova [p], E. Drago [z], D. Duchesneau [q], P. Duinker [b], I. Duran [ak], S. Easo [ae], H. El Mamouni [v], A. Engler [af], F.J. Eppling [m], F.C. Erné [b], P. Extermann [q], R. Fabbretti [aq], M. Fabre [aq], S. Falciano [ah], S.J. Fan [aℓ], O. Fackler [t], J. Fay [v], M. Felcini [o], T. Ferguson [af], D. Fernandez [w], G. Fernandez [w], F. Ferroni [ah], H. Fesefeldt [a], E. Fiandrini [ae], J. Field [q], F. Filthaut [ab], G. Finocchiaro [ah], P.H. Fisher [e], G. Forconi [q], T. Foreman [b], K. Freudenreich [as], W. Friebel [ar], M. Fukushima [m], M. Gailloud [s], Yu. Galaktionov [y,m], E. Gallo [n], S.N. Ganguli [o,h], P. Garcia-Abia [w], D. Gele [v], S. Gentile [ah,o], S. Goldfarb [j], Z.F. Gong [r], E. Gonzalez [w], A. Gougas [e], D. Goujon [q], G. Gratta [ad], M. Gruenewald [ad], C. Gu [p], M. Guanziroli [p], J.K. Guo [aℓ], V.K. Gupta [ag], A. Gurtu [h], H.R. Gustafson [c], L.J. Gutay [ap], K. Hangarter [a], A. Hasan [p], D. Hauschildt [b], C.F. He [aℓ], J.T. He [f], T. Hebbeker [a], M. Hebert [aj], G. Herten [m], A. Hervé [o], K. Hilgers [a], H. Hofer [as], H. Hoorani [q], G. Hu [p], G.Q. Hu [aℓ], B. Ille [v], M.M. Ilyas [p], V. Innocente [o], H. Janssen [o], S. Jezequel [d], B.N. Jin [f], L.W. Jones [c], A. Kasser [s], R.A. Khan [p], Yu. Kamyshkov [ac], P. Kapinos [ai,ar], J.S. Kapustinsky [u], Y. Karyotakis [o], M. Kaur [p], S. Khokhar [p], M.N. Kienzle-Focacci [q], J.K. Kim [an], S.C. Kim [an], Y.G. Kim [an], W.W. Kinnison [u], A. Kirkby [ad], D. Kirkby [ad], S. Kirsch [ar], W. Kittel [ab], A. Klimentov [m,y], A.C. König [ab], E. Koffeman [b], O. Kornadt [a], V. Koutsenko [m,y], A. Koulbardis [ai], R.W. Kraemer [af], T. Kramer [m], V.R. Krastev [am,ae], W. Krenz [a], A. Krivshich [ai], H. Kuijten [ab], K.S. Kumar [ℓ], A. Kunin [m,y], G. Landi [n], D. Lanske [a], S. Lanzano [z], P. Lebrun [v], P. Lecomte [as], P. Lecoq [o], P. Le Coultre [as], D.M. Lee [u], I. Leedom [j], C. Leggett [c], J.M. Le Goff [o], R. Leiste [ar], M. Lenti [n], E. Leonardi [ah], X. Leytens [b], C. Li [r,p], H.T. Li [f], P.J. Li [aℓ], J.Y. Liao [aℓ], W.T. Lin [au], Z.Y. Lin [r], F.L. Linde [o], B. Lindemann [a], L. Lista [z], Y. Liu [p], W. Lohmann [ar,o], E. Longo [ah], Y.S. Lu [f], J.M. Lubbers [o], K. Lübelsmeyer [a], C. Luci [ah], D. Luckey [g,m], L. Ludovici [ah], L. Luminari [ah], W. Lustermann [ar], J.M. Ma [f], W.G. Ma [r], M. MacDermott [as],

P.K. Malhotra [h,3], R. Malik [p], A. Malinin [y], C. Maña [w], M. Maolinbay [as], P. Marchesini [as], F. Marion [d], A. Marin [i], J.P. Martin [v], L. Martinez-Laso [w], F. Marzano [ah], G.G.G. Massaro [b], K. Mazumdar [h], P. McBride [ℓ], T. McMahon [ap], D. McNally [as], M. Merk [af], L. Merola [z], M. Meschini [n], W.J. Metzger [ab], Y. Mi [s], G.B. Mills [u], Y. Mir [p], G. Mirabelli [ah], J. Mnich [a], M. Möller [a], B. Monteleoni [n], R. Morand [d], S. Morganti [ah], N.E. Moulai [p], R. Mount [ad], S. Müller [a], A. Nadtochy [ai], E. Nagy [k], M. Napolitano [z], F. Nessi-Tedaldi [as], H. Newman [ad], C. Neyer [as], M.A. Niaz [p], A. Nippe [a], H. Nowak [ar], G. Organtini [ah], D. Pandoulas [a], S. Paoletti [n], P. Paolucci [z], G. Pascala [ah], G. Passaleva [n,ae], S. Patricelli [z], T. Paul [e], M. Pauluzzi [ae], C. Paus [a], F. Pauss [as], Y.J. Pei [a], S. Pensotti [x], D. Perret-Gallix [d], J. Perrier [q], A. Pevsner [e], D. Piccolo [z], M. Pieri [o], P.A. Piroué [ag], F. Plasil [ac], V. Plyaskin [y], M. Pohl [as], V. Pojidaev [y,n], H. Postema [m], Z.D. Qi [aℓ], J.M. Qian [c], K.N. Qureshi [p], R. Raghavan [h], G. Rahal-Callot [as], P.G. Rancoita [x], M. Rattaggi [x], G. Raven [b], P. Razis [aa], K. Read [ac], D. Ren [as], Z. Ren [p], M. Rescigno [ah], S. Reucroft [j], A. Ricker [a], S. Riemann [ar], B.C. Riemers [ap], K. Riles [c], O. Rind [c], H.A. Rizvi [p], F.J. Rodriguez [w], B.P. Roe [c], M. Röhner [a], S. Röhner [a], L. Romero [w], J. Rose [a], S. Rosier-Lees [d], R. Rosmalen [ab], Ph. Rosselet [s], W. van Rossum [b], S. Roth [a], A. Rubbia [m], J.A. Rubio [o], H. Rykaczewski [as], M. Sachwitz [ar], J. Salicio [o], J.M. Salicio [w], G.S. Sanders [u], A. Santocchia [ae], M.S. Sarakinos [m], G. Sartorelli [g,p], M. Sassowsky [a], G. Sauvage [d], C. Schäfer [a], V. Schegelsky [ai], D. Schmitz [a], P. Schmitz [a], M. Schneegans [d], H. Schopper [at], D.J. Schotanus [ab], S. Shotkin [m], H.J. Schreiber [ar], J. Shukla [af], R. Schulte [a], S. Schulte [a], K. Schultze [a], J. Schwenke [a], G. Schwering [a], C. Sciacca [z], I. Scott [ℓ], R. Sehgal [p], P.G. Seiler [aq], J.C. Sens [o,b], L. Servoli [ae], I. Sheer [aj], D.Z. Shen [aℓ], S. Shevchenko [ad], X.R. Shi [ad], E. Shumilov [y], V. Shoutko [y], D. Son [an], A. Sopczak [aj], C. Spartiotis [e], T. Spickermann [a], P. Spillantini [n], R. Starosta [a], M. Steuer [g,m], D.P. Stickland [ag], F. Sticozzi [m], H. Stone [ag], K. Strauch [ℓ], B.C. Stringfellow [ap], K. Sudhakar [h], G. Sultanov [p], L.Z. Sun [r,p], H. Suter [as], J.D. Swain [p], A.A. Syed [ab], X.W. Tang [f], L. Taylor [j], G. Terzi [x], Samuel C.C. Ting [m], S.M. Ting [m], M. Tonutti [a], S.C. Tonwar [h], J. Tóth [k], A. Tsaregorodtsev [ai], G. Tsipolitis [af], C. Tully [ag], K.L. Tung [f], J. Ulbricht [as], L. Urbán [k], U. Uwer [a], E. Valente [ah], R.T. Van de Walle [ab], I. Vetlitsky [y], G. Viertel [as], P. Vikas [p], U. Vikas [p], M. Vivargent [d], H. Vogel [af], H. Vogt [ar], I. Vorobiev [y], A.A. Vorobyov [ai], L. Vuilleumier [s], M. Wadhwa [d], W. Wallraff [a], C. Wang [m], C.R. Wang [r], G.H. Wang [af], X.L. Wang [r], Y.F. Wang [m], Z.M. Wang [p,r], A. Weber [a], J. Weber [as], R. Weill [s], T.J. Wenaus [t], J. Wenninger [q], M. White [m], C. Willmott [w], F. Wittgenstein [o], D. Wright [ag], S.X. Wu [p], S. Wynhoff [a], B. Wysłouch [m], Y.Y. Xie [aℓ], J.G. Xu [f], Z.Z. Xu [r], Z.L. Xue [aℓ], D.S. Yan [aℓ], B.Z. Yang [r], C.G. Yang [f], G. Yang [p], C.H. Ye [p], J.B. Ye [r], Q. Ye [p], S.C. Yeh [au], Z.W. Yin [aℓ], J.M. You [p], N. Yunus [p], M. Yzerman [b], C. Zaccardelli [ad], P. Zemp [as], M. Zeng [p], Y. Zeng [a], D.H. Zhang [b], Z.P. Zhang [r,p], B. Zhou [i], G.J. Zhou [f], J.F. Zhou [a], R.Y. Zhu [ad], A. Zichichi [g,o,p] and B.C.C. van der Zwaan [b]

[a] *I. Physikalisches Institut, RWTH, W-5100 Aachen, FRG* [1]
and III. Physikalisches Institut, RWTH, W-5100 Aachen, FRG [1]
[b] *National Institute for High Energy Physics, NIKHEF, NL-1009 DB Amsterdam, The Netherlands*
[c] *University of Michigan, Ann Arbor, MI 48109, USA*
[d] *Laboratoire d'Annecy-le-Vieux de Physique des Particules, LAPP,IN2P3-CNRS, BP 110, F-74941 Annecy-le-Vieux Cedex, France*
[e] *Johns Hopkins University, Baltimore, MD 21218, USA*
[f] *Institute of High Energy Physics, IHEP, 100039 Beijing, China*
[g] *INFN-Sezione di Bologna, I-40126 Bologna, Italy*
[h] *Tata Institute of Fundamental Research, Bombay 400 005, India*
[i] *Boston University, Boston, MA 02215, USA*
[j] *Northeastern University, Boston, MA 02115, USA*
[k] *Central Research Institute for Physics of the Hungarian Academy of Sciences, H-1525 Budapest 114, Hungary* [2]
[ℓ] *Harvard University, Cambridge, MA 02139, USA*

[m] *Massachusetts Institute of Technology, Cambridge, MA 02139, USA*
[n] *INFN Sezione di Firenze and University of Florence, I-50125 Florence, Italy*
[o] *European Laboratory for Particle Physics, CERN, CH-1211 Geneva 23, Switzerland*
[p] *World Laboratory, FBLJA Project, CH-1211 Geneva 23, Switzerland*
[q] *University of Geneva, CH-1211 Geneva 4, Switzerland*
[r] *Chinese University of Science and Technology, USTC, Hefei, Anhui 230 029, China*
[s] *University of Lausanne, CH-1015 Lausanne, Switzerland*
[t] *Lawrence Livermore National Laboratory, Livermore, CA 94550, USA*
[u] *Los Alamos National Laboratory, Los Alamos, NM 87544, USA*
[v] *Institut de Physique Nucléaire de Lyon, IN2P3-CNRS, Université Claude Bernard, F-69622 Villeurbanne Cedex, France*
[w] *Centro de Investigaciones Energeticas, Medioambientales y Tecnologicas, CIEMAT, E-28040 Madrid, Spain*
[x] *INFN-Sezione di Milano, I-20133 Milan, Italy*
[y] *Institute of Theoretical and Experimental Physics, ITEP, Moscow, Russian Federation*
[z] *INFN-Sezione di Napoli and University of Naples, I-80125 Naples, Italy*
[aa] *Department of Natural Sciences, University of Cyprus, Nicosia, Cyprus*
[ab] *University of Nymegen and NIKHEF, NL-6525 ED Nymegen, The Netherlands*
[ac] *Oak Ridge National Laboratory, Oak Ridge, TN 37831, USA*
[ad] *California Institute of Technology, Pasadena, CA 91125, USA*
[ae] *INFN-Sezione di Perugia and Universitá Degli Studi di Perugia, I-06100 Perugia, Italy*
[af] *Carnegie Mellon University, Pittsburgh, PA 15213, USA*
[ag] *Princeton University, Princeton, NJ 08544, USA*
[ah] *INFN-Sezione di Roma and University of Rome, "La Sapienza", I-00185 Rome, Italy*
[ai] *Nuclear Physics Institute, St. Petersburg, Russian Federation*
[aj] *University of California, San Diego, CA 92093, USA*
[ak] *Dept. de Fisica de Particulas Elementales, Univ. de Santiago, E-15706 Santiago de Compostela, Spain*
[aℓ] *Shanghai Institute of Ceramics, SIC, Shanghai, China*
[am] *Bulgarian Academy of Sciences, Institute of Mechatronics, BU-1113 Sofia, Bulgaria*
[an] *Center for High Energy Physics, Korea Advanced Inst. of Sciences and Technology, 305-701 Taejon, South Korea*
[ao] *University of Alabama, Tuscaloosa, AL 35486, USA*
[ap] *Purdue University, West Lafayette, IN 47907, USA*
[aq] *Paul Scherrer Institut, PSI, CH-5232 Villigen, Switzerland*
[ar] *DESY-Institut für Hochenergiephysik, O-1615 Zeuthen, FRG*
[as] *Eidgenössische Technische Hochschule, ETH Zürich, CH-8093 Zürich, Switzerland*
[at] *University of Hamburg, W-2000 Hamburg, FRG*
[au] *High Energy Physics Group, Taiwan*

Received 31 March 1993
Editor: K. Winter

We report a measurement of $R_b = \Gamma_{b\bar{b}}/\Gamma_{had}$ from $Z \to q\bar{q}$ events at LEP. $Z \to b\bar{b}$ events are identified using a multidimensional analysis based on a neural network approach. We obtain 60% sample purity with an efficiency of 35%. Our measured value of R_b is $0.222 \pm 0.003 \pm 0.007$.

1. Introduction

The measurement of the partial decay width of Z into bb, $\Gamma_{b\bar{b}}$, at LEP, provides an important test of the validity of the Standard Model (SM) [1] and allows a precise determination of the neutral current couplings to b quarks. With high statistics and precision, the measurement is sensitive to deviations from the one loop prediction of the SM and may give hints of new physics.

For $\Gamma_{b\bar{b}}$, radiative corrections are two-fold, the oblique correction to the gauge boson propagator, $\Delta\rho$, and the one loop correction to the $Zb\bar{b}$ vertex coming from virtual t–W exchange. These correc-

[1] Supported by the German Bundesministerium für Forschung und Technologie.
[2] Supported by the Hungarian OTKA fund under contract number 2970.
[3] Deceased.

tions are sensitive to the top quark mass and are less sensitive to the Higgs mass. The oblique correction affects all the partial decay widths of Z into fermions while the vertex correction is specific to decays into $b\bar{b}$. The ratio

$$R_b = \Gamma_{b\bar{b}}/\Gamma_{had} \quad (1)$$

has a contribution from the vertex correction $Zb\bar{b}$ and is free from $\Delta\rho$ as well as from QCD and Higgs mass effects. It can give a clean constraint on the top mass within the SM [2] provided it is known to better than one percent.

In this paper we present a measurement of R_b from hadronic decays of the Z collected with the L3 detector. The selection of $b\bar{b}$ events and their discrimination from other hadronic events is performed using a multidimensional analysis based on a neural network approach. In contrast to our previous measurement [3], we use the entire hadronic sample without requiring a semileptonic decay and so are not limited by the knowledge of the semileptonic branching ratio.

The neural network method has proven to be very effective for event classification in a complex pattern environment [4,5] and is being increasingly used in high energy physics [6,7].

2. The L3 detector

The L3 detector covers 99% of 4π. The detector consists of a central tracking chamber, a high resolution electromagnetic calorimeter composed of BGO crystals, a ring of scintillation counters, a uranium and brass hadron calorimeter with proportional wire chamber readout, and a precise muon spectrometer. These detectors are installed in a 12 m diameter magnet which provides a uniform field of 0.5 T along the beam direction. A detailed description of each detector subsystem, and its performance, is given in ref. [8].

The fine segmentation of the electromagnetic and the hadron calorimeter allows us to measure the direction of jets with an angular resolution of 2.5°, and to measure the total energy of hadronic events from Z decay with a resolution of 10.2%. For the present analysis, we use the data collected in the polar angular ranges of $5° < \theta < 175°$ for the hadron calorimeter and $11° < \theta < 169°$ for the electromagnetic calorimeter.

3. Hadron event selection

Events of the type $e^+e^- \rightarrow$ hadrons are selected by requiring:
- $0.45 < E_{vis}/\sqrt{s} < 1.4$;
- $|E_\parallel|/E_{vis} < 0.5$;
- $E_\perp/E_{vis} < 0.5$;
- $N_{cluster} > 18$;
- at least two jets with $E_{jet} > 10$ GeV and a minimum of four clusters in each jet.

E_{vis} is the total visible energy in the detector. $|E_\parallel|$ and $E_\perp$ are the parallel and transverse energy imbalances. $N_{cluster}$ is the number of clusters with energy greater than 100 MeV. The cluster and jet reconstruction proceeds using a two step pattern recognition algorithm [9] which groups adjacent energy depositions in the electromagnetic and the hadron calorimeters into clusters and then collects these clusters into jets. Typically each cluster represents a single particle (hadron, electron, photon). The direction of the cluster is defined by the energy weighted vector sum of all the hits that belong to it. The purpose of the above criteria is to keep only $Z \rightarrow q\bar{q}$ events and reject all e^+e^-, $\mu^+\mu^-$, $\tau^+\tau^-$, and two-photon hadron production to better than 0.1%.

For the present analysis we select 238 000 $Z \rightarrow q\bar{q}$ events collected with the L3 detector during 1991 LEP running on the Z peak.

We use a sample of Monte Carlo events based on JETSET7.3 [10] with parton shower fragmentation. The response of the detector is simulated using the L3 simulation program [11]. The simulated events are then reconstructed by the same reconstruction program as that used for the data.

4. Identification of bb events

Because the b quark is heavy, $b\bar{b}$ events can be distinguished from events containing lighter quarks. A standard method is to use the high momentum leptons coming from the semileptonic decays of b quarks. We present here a different method which relies on

the general properties of the $b\bar{b}$ events, rather than exclusively on their semileptonic decays.

In the hadronization of a b quark, very little energy is radiated in the form of gluons. Thus, the resulting b hadron carries off a large fraction of the beam energy, typically 70%. It then decays into several particles in a weak decay process. In contrast, most of the energy from a light quark is radiated out in the form of gluons leading to a broad energy spectrum of particles. Thus, the energy gaps between the leading particles are larger for light quark jets. Also the leading light hadron being stable can still be fairly energetic. So, by comparing the energies of the leading particles, as well as the differences in energies of particles within a jet, one can distinguish between b quark and lighter quark jets. In addition, the mass of the b quark affects the jet characteristics. Jets from b quarks are typically broader than light quark jets. The jet boost ($\gamma\beta = p/m$) is also smaller for b quark jets.

None of the above properties alone is sufficient to select a sample of $b\bar{b}$ events with high purity and good efficiency. However, when used in a multidimensional analysis which exploits the correlations between them, a high selection efficiency with good sample purity can be achieved.

We consider five variables, described below, for each of the two most energetic jets of the event. The information used is based only on the calorimetric clusters. All clusters with energy exceeding 100 MeV within 30° of the jet axis are used and the jet energy, invariant mass and the jet direction are redefined on the basis of these clusters. The discriminating features of the variables are checked using data. For this purpose we use $b\bar{b}$ events tagged by high p_t(> 1 GeV) muons, where p_t is the momentum of the muon transverse to the jet axis. To avoid biases, we use the jet opposite the muon-tagged jet for studying the variables.

The variables that we use are:

(1) The $\gamma\beta$ of the jet using the jet energy and the invariant mass determined by the clusters, where the clusters are assumed to be massless. In fig. 1a we show the $\gamma\beta$ distribution for the most energetic jet for the data compared to the Monte Carlo. In fig. 1b the distribution for all data is compared with that for jets opposite to a muon-tagged jet. Both the data and the Monte Carlo show that b jets tend to have smaller $\gamma\beta$ value than light quark jets.

(2) The energy of the most energetic cluster which tends to be lower for $b\bar{b}$ events than for light quark events.

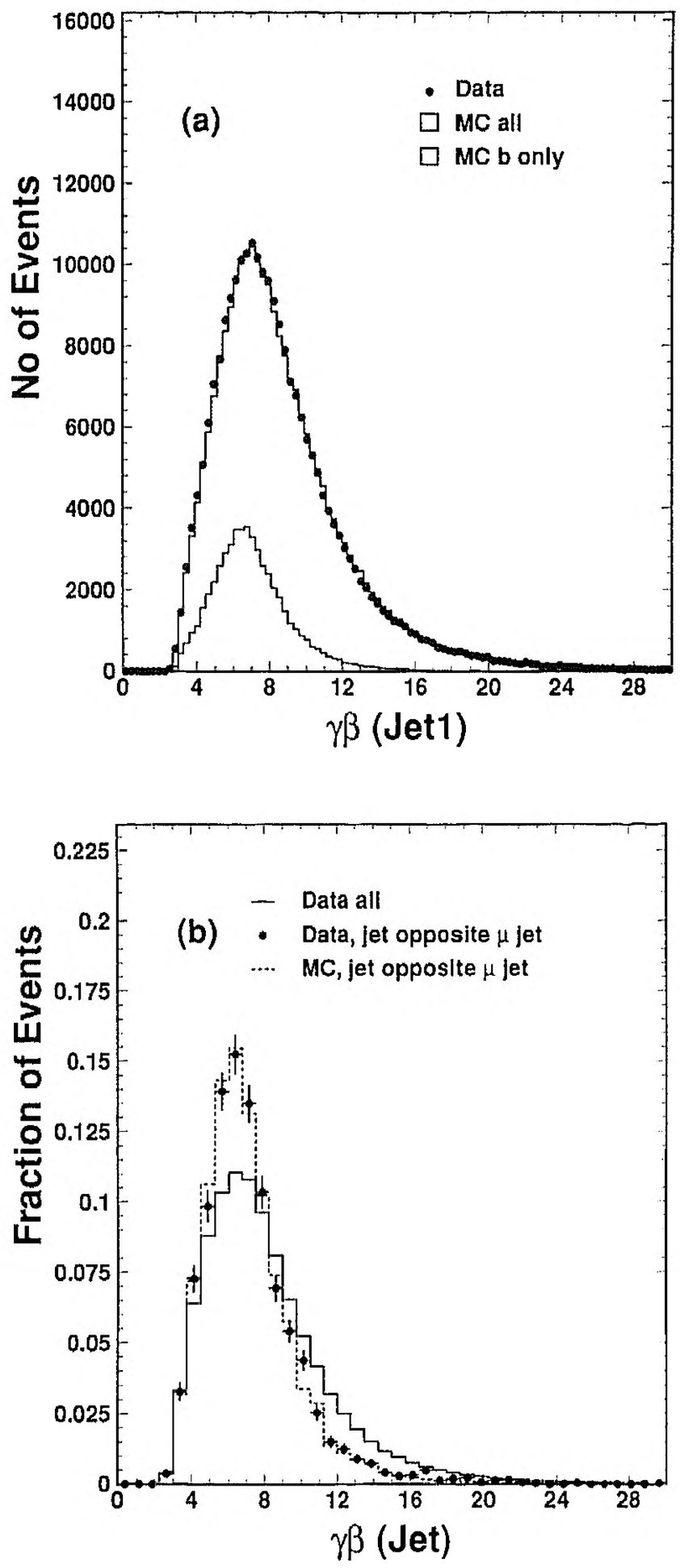

Fig. 1. The distribution of $\gamma\beta$ for (a) the most energetic jet compared to the Monte Carlo, and for (b) the muon tagged sample compared to all data.

(3) The directed sphericity of the jet defined as

$$S_{\mathrm{dir}} = \frac{\sum p_{\perp}^2}{\sum p^2},$$

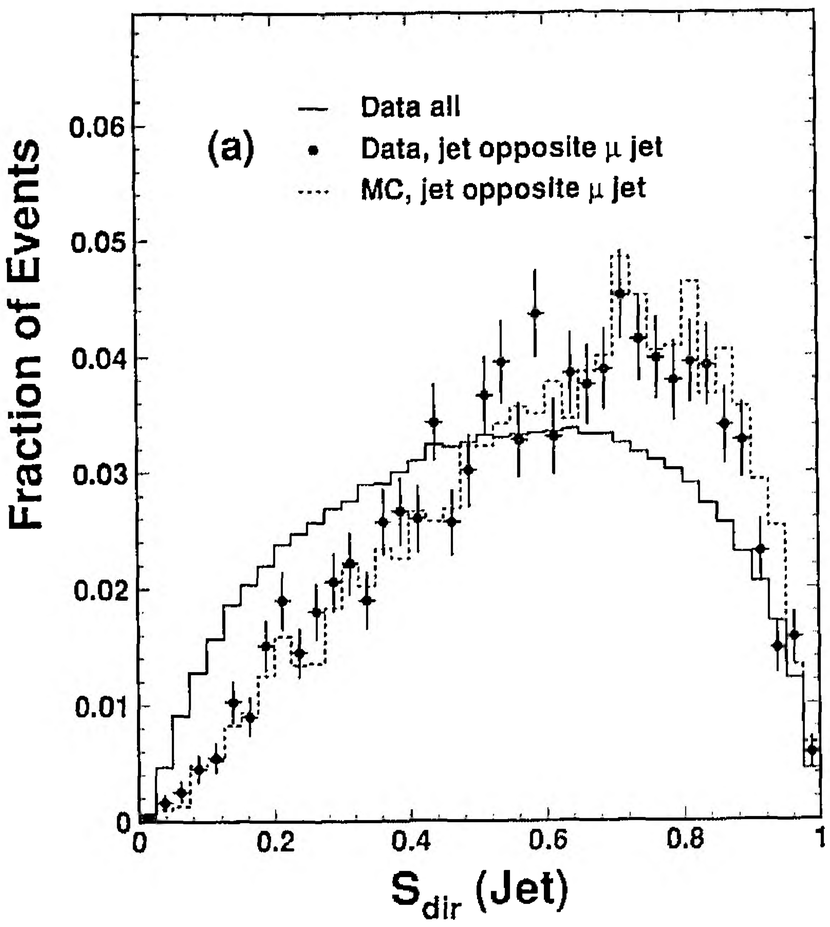

Fig. 2. (a) The directed sphericity distribution for all jets compared to the muon-tagged sample and (b) the energy gap between the most energetic and fourth most energetic clusters for all jets compared to the the muon-tagged sample.

where the momenta are in the jet rest frame, and the transverse direction is with respect to the jet direction. Fig. 2a shows the distribution for all data compared to the muon-tagged events.

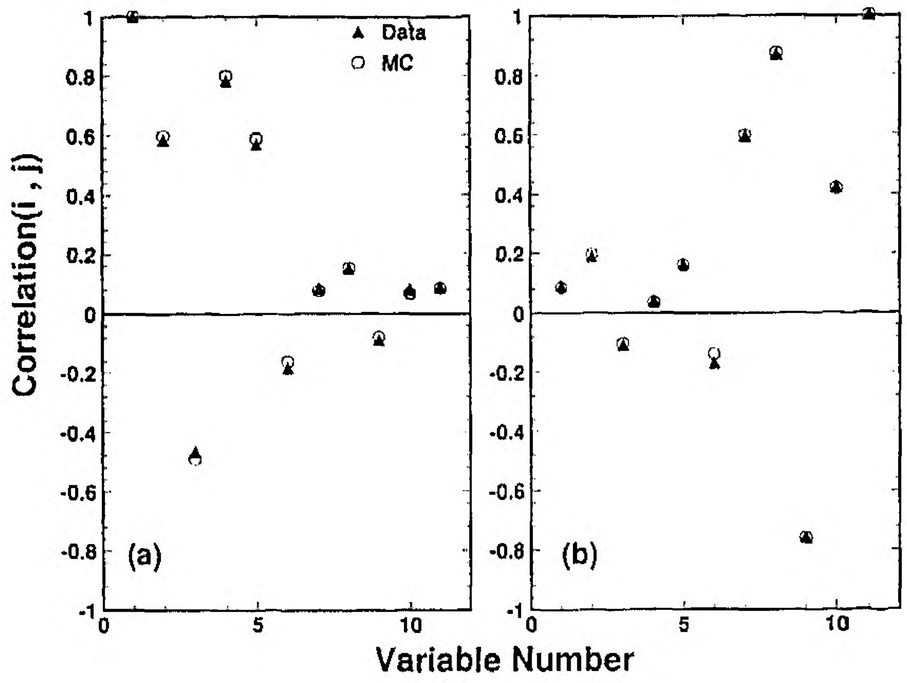

Fig. 3. The correlation coefficient (a) between $\gamma\beta$ of the most energetic jet and all other quantities and (b) between the energy gap of the second jet and all other quantities. The quantites are labelled 1–5 for the most energetic jet, 7–11 for the second most energetic jet, and 6 for the global event quantity, E_{left}.

(4) The $\gamma\beta$ of the set of the four leading clusters in the jet.

(5) The energy gap between the first and the fourth most energetic clusters, E_{gap}, scaled by the jet energy. In fig. 2b we plot this distribution for all jets compared to the muon-tagged sample.

In addition we use the global variable E_{lcft} defined as the fraction of visible energy outside the two most energetic jets:

$$E_{\text{left}} = \frac{E_{\text{vis}} - (E_{\text{jet1}} + E_{\text{jet2}})}{E_{\text{vis}}},$$

where E_{jet1} and E_{jet2} are the energies of the two jets. Although the distribution of E_{left} for b and non-b events is similar, the correlation between it and other variables is useful in a multidimensional analysis.

Altogether, 11 variables are used per event.

Figs. 1 and 2 show that the Monte Carlo describes the data well. Before performing the multidimensional analysis of these quantities, we have also checked that their correlations with each other are in good agreement. In fig. 3 we show, as an example, the correlation between $\gamma\beta$ for the most energetic jet and all other quantities, and between the energy gap of the second jet and the other quantities. One can also see that variables within the same jet have stronger correlations compared to those in different jets.

5. The multidimensional analysis

Multidimensional analysis for event classification exploits the correlations between the various quantities that characterize the events. For every event the characterizing quantities can be considered as a vector $\boldsymbol{x}$ $(x_1, x_2, ..., x_N)$. In our particular case, the vector $\boldsymbol{x}$ has the 11 quantities described above as components. We then determine the classifier function $F_c(\boldsymbol{x}, \boldsymbol{w})$ to separate b quark events from non-b quark events. The vector $\boldsymbol{w}$ is a vector of weights adjusted to minimize the classification error

$$\int | F_c(\boldsymbol{x}, \boldsymbol{w}) - F_{\text{known}}(\boldsymbol{x}) |^2 \rho(\boldsymbol{x}) \, d\boldsymbol{x} ,$$

where $\rho(\boldsymbol{x})$ is the density function of the events and F_{known} the classifier function known from Monte Carlo. The determination of the weight vector ("training") is performed using Monte Carlo events. The probability distribution of the classifier $F_c(\boldsymbol{x}, \boldsymbol{w})$ for Monte Carlo events is expected to agree with the data provided that $\rho_{\text{MC}}(\boldsymbol{x}) = \rho_{\text{data}}(\boldsymbol{x})$.

In a conventional neural network [4,5], the classifier function is derived from successive layers of neurons. Each neuron gets as input a linear sum of the quantities of the previous layer and provides as output a non-linear transformation of the linear sum. In the less conventional approach that we follow [5], the input variables are first expanded using orthonormal functions. A simple summation of the transformed variables is used in only one non-linear transformation. This eliminates the intermediate stages and reduces the number of weights.

Each input quantity, x_k is first scaled to be in the range $(-1, 1)$. It is then expanded using the functional transform $f(x_k)$ given by

$$f(x_k) = w_{1k} x_k + \sum_{j=1}^{n} (w_{2kj} \sin(j\pi x_k) + w_{3kj} \cos(j\pi x_k)) . \quad (2)$$

For our purposes, we have determined that $n = 4$ is an optimal choice for the performance of the network. The transformed input quantities are then summed to form

$$X = \sum_{k=1}^{11} f(x_k) + w_0 . \quad (3)$$

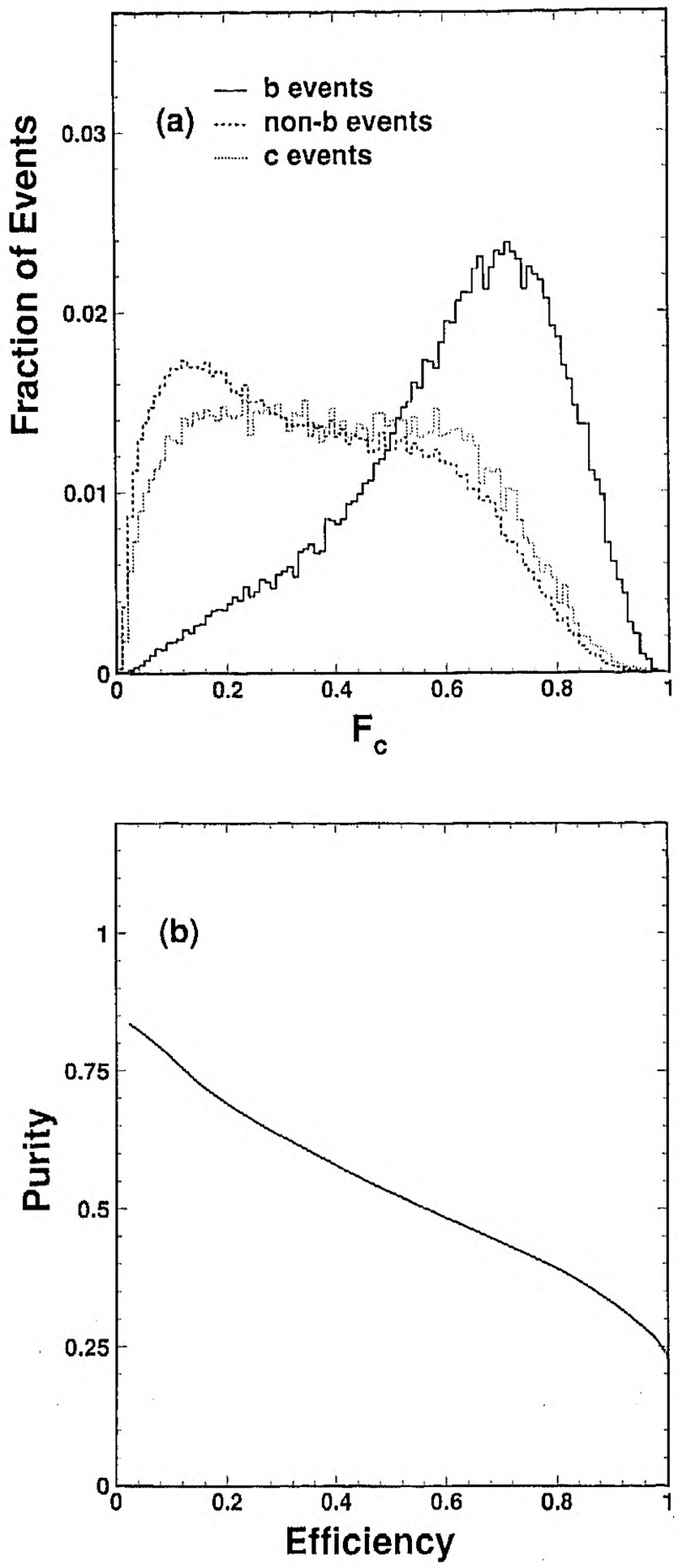

Fig. 4. (a) The network response for b events and non-b events separately. (b) Purity and efficiency of the classifier function for b events.

The classifier function used is

$$F_c(X) = \frac{1}{1 + e^{-X}} \equiv F_c(\boldsymbol{x}, \boldsymbol{w}) . \quad (4)$$

We determine the weights $\boldsymbol{w}$ with a sample of 150 000 Monte Carlo events to minimize

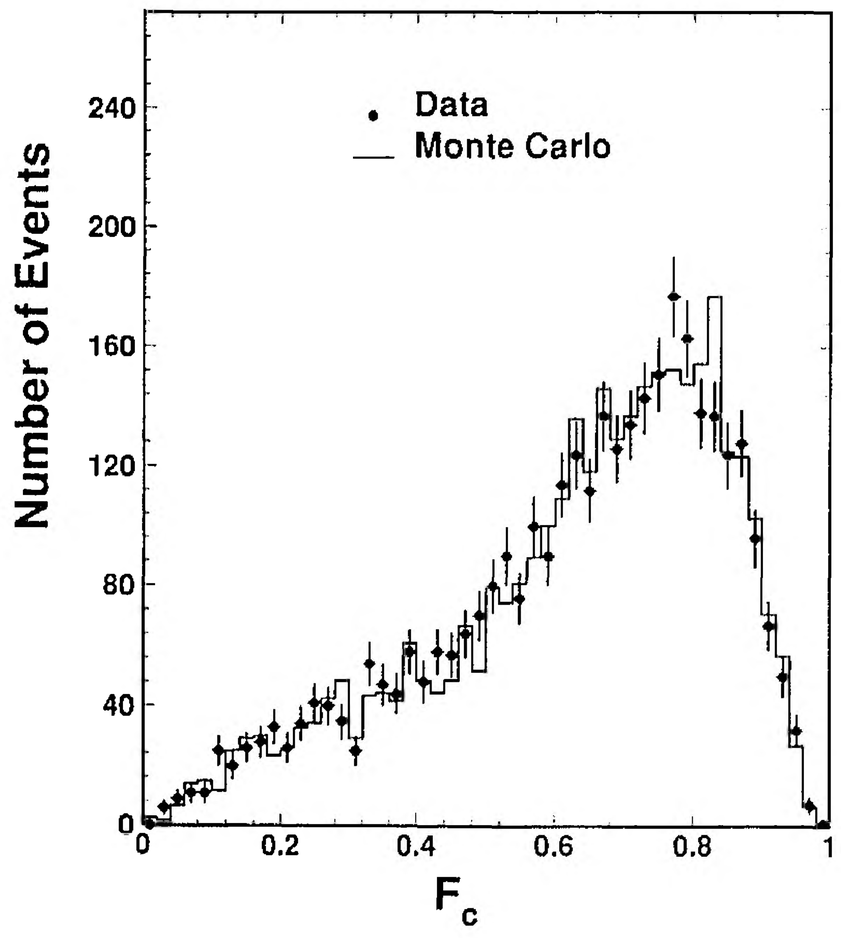

Fig. 5. The network response for events tagged by a high p_t muon for the data compared to the Monte Carlo.

$$[F_c(x, w) - F_{\text{known}}]^2 , \qquad (5)$$

where F_{known} is chosen to be 0.025 for non-b and 0.975 for b events. The discriminating power of the classifier function is then tested using an independent sample of 200 000 Monte Carlo events.

The network classifier response for the Monte Carlo test sample is shown in fig. 4a. The b events dominate at larger values of F_c and the non-b at smaller values. Fig. 4b shows the b sample purity as a function of the tagging efficiency. As an example of the performance of the network, we achieve 35% efficiency for 60% purity. For high purities the efficiency is approximately a factor two better than those in similar studies [7].

In order to test the network reliability and to make sure that the correlations among the different variables both in the Monte Carlo and the data are well understood, the response of the network which has been trained using Monte Carlo $q\bar{q}$ events is compared for those events that have a high p_t (> 1 GeV) muon (fig. 5). The whole event is used but no information from the muons themselves is used in the network. These events are approximately 80% $b\bar{b}$ [12]. The Monte Carlo reproduces well the data. This indicates that the correlations among the different variables used are well simulated in the Monte Carlo and it does represent the data in detail. An important point to note is that the high p_t muon events are distributed in the entire range of F_c in much the same way as all other b events indicating that the high purity sample of b events from the network are not just from the semileptonic decays of b hadrons. Thus the uncertainty in the semileptonic branching ratio of b quark has an insignificant effect on the network results.

6. Determination of $\Gamma_{b\bar{b}}/\Gamma_{had}$

To determine $R_b = \Gamma_{b\bar{b}}/\Gamma_{had}$, we perform a fit to the data distribution of F_c by varying the b and non-b contribution from the Monte Carlo. In fig. 6 we compare the data with the fitted distribution and also plot the b and non-b contributions. We determine $\Gamma_{b\bar{b}}/\Gamma_{had} = 0.222 \pm 0.003$. The error includes the statistical error due to the Monte Carlo test sample. We obtain similar results using a simpler procedure of applying a cut on the value of the classifier depending upon the desired sample purity and the tagging efficiency.

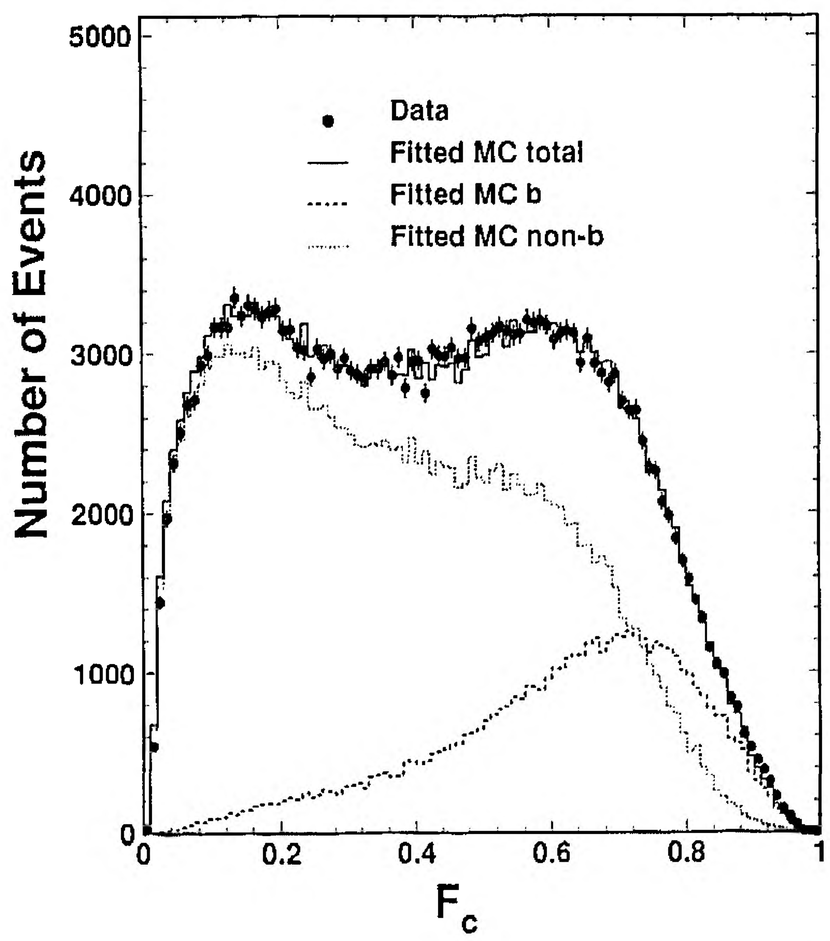

Fig. 6. Fit of the network response to the data. Also shown is the response for b and non-b events separately.

Table 1
Summary of the systematic errors due to various sources.

Source of systematic error	Variation	ΔR_b
$b \to \ell\nu X$ branching ratio	0.02	0.0010
b quark fragmentation parameter ϵ_b	0.004	0.0031
c quark fragmentation parameter ϵ_c	0.02	0.0018
Λ_{LL} (GeV) the shower scale parameter	0.03	0.0037
b (GeV^{-2}) parameter in Lund sym. fragmentation	0.08	0.0024
σ_q (GeV), Gaussian p_t width of hadrons	0.03	0.0022
mass of the b quark (GeV)	0.5	0.0006
$\Gamma_{c\bar{c}}$ (MeV)	15	0.0011
change in energy resolution of the calorimeter $\Delta\sigma(E)$	10%	0.0020
total uncertainty from all sources		0.007

As we use Monte Carlo events to describe the data and estimate the different acceptances, there are several parameters that affect the event description. Details of the various parameters used in the Monte Carlo and the different fragmentation schemes is given in ref. [13]. For the light u, d, and s quarks the Lund symmetric fragmentation function is used while for b and c quarks the Peterson fragmentation function [14] is used. For estimating the systematic error each parameter is varied by its error [13] and a new test sample is generated. Comparing the sample purity and tagging efficiency of the new test sample with the standard test sample the change in R_b is estimated. For this purpose fast simulations using approximate detector resolutions have been made. The changes in R_b for different parameters are given in table 1. In addition to the QCD parameters we have changed the semileptonic branching ratio of b hadrons and varied the detector response. Adding all the systematic errors in quadrature, we arrive at the total systematic error on R_b of 0.007.

7. Conclusions

We have identified $b\bar{b}$ events in Z hadronic decays using a multidimensional analysis with several variables which characterize the event topology. A neural network based on functional expansion provides a very good separation between b and non-b events. We achieve high sample purity of $b\bar{b}$ events with good tagging efficiency: for 60% sample purity we obtain 35% efficiency. From a fit to the full range of the classifier function, we determine:

$$R_b = 0.222 \pm 0.003 \pm 0.007.$$

This result is a significant improvement of our previous measurement [3], $R_b = 0.218 \pm 0.004 \pm 0.012$, using only the semileptonic decays, and is in good agreement with the Standard Model value $R_b = 0.216$ computed with a top mass of 150 GeV.

Acknowledgement

We wish to express our gratitude to the CERN accelerator divisions for the excellent performance of the LEP machine. We acknowledge the efforts of all engineers and technicians who have participated in the construction and maintenance of this experiment.

References

[1] S. L. Glashow, Nucl. Phys. 22 (1961) 579;
S. Weinberg, Phys. Rev. Lett. 19 (1967) 1264;
A. Salam, Elementary Particle Theory, Ed. N. Svartholm, Stockholm, Almquist and Wiksell (1968) p. 367.
[2] A. Djouadi et al., Nucl. Phys. B 349 (1991) 48;
F. Boudjema et al., Phys. Lett. B 238 (1990) 423;
G. Girardi et al., Phys. Lett. B 240 (1990) 492;
F. M. Renard and C. Verzegnassi, Phys. Lett. B 260 (1991) 225;
J. Layssac et al., Phys. Lett. B 287 (1992) 267;
A. Blondel et al., Phys. Lett. B 293 (1992)253.
[3] L3 Collab., B. Adeva et al., Phys. Lett. B 261 (1991) 177.

[4] R. Hecht-Nielsen, Theory of Back Propagation Neural Network, Proc. Int. Joint Conf. on Neural Networks I, 593, IEEE Press, New York (1989); Neurocomputing, Addison-Wesley Publishing Company (1990).
B. Denby, Tutorial on Neural Network Applications in High Energy Physics: A 1992 Perspective, Fermilab Preprint, FERMILAB-Conf-92/121-E.
R. Beale and T. Jackson, Neural Computing: An Introduction, Adam Hilger Publishing, Bristol (1990).
[5] Y.-H. Pao, Adaptive Pattern Recognition and Neural Networks, Addison-Wesley Publishing Company (1989).
[6] V. Innocente, Y. F. Wang and Z. P. Zhang, Nucl. Instrum. Methods A 323 (1992) 647;
L. Lönnblad et al., Nucl. Phys. B 349 (1991) 675.
[7] C. Bortolotto et al., Nucl. Instrum. Methods A 306 (1991) 459;
L. Bellantoni et al., Nucl. Instrum. Methods A 310 (1991) 618;
DELPHI Collab., P. Abreu et al., Phys. Lett. B 295 (1992) 383;
P. Mazzanti and R. Odorico, Bologna preprint DFUB 92/15 (1992).
[8] L3 Collab., B. Adeva et al., Nucl. Instrum. Methods A 289 (1990) 35.
[9] O. Adriani et al., Nucl. Instrum. Methods A 302 (1991) 53;
L3 Collab., B. Adeva et al., Phys. Lett. B 248 (1990) 227; 464.
[10] T. Sjöstrand and M. Bengtsson, Comput. Phys. Commun. 43 (1987) 367;
T. Sjöstrand, Z Physics at LEP, CERN report CERN-89-08, Vol. III, Eds. G. Altarelli, R. Kleiss and C. Verzegnassi (CERN, Geneva, 1989) p. 143.
[11] The L3 detector simulation is based on GEANT Version 3.14,
see R. Brun et al., GEANT 3, CERN DD/EE/84-1 (Revised), September 1987;
the GHEISHA program (H. Fesefeldt, RWTH Aachen Preprint PITHA 85/02 (1985)) is used to simulate hadronic interactions.
[12] L3 Collab., O. Adriani et al., Phys. Lett. B 292 (1992) 454.
[13] L3 Collab., B. Adeva et al., Z. Phys. C 55 (1992) 39.
[14] C. Peterson et al., Phys. Rev. D 27 (1983) 105.